

Frequency and Peak Stretch Magnitude Affect Alveolar Epithelial Permeability

Taylor S. Cohen, Kenneth J. Cavanaugh, and Susan S. Margulies

Department of Bioengineering, University of Pennsylvania, Philadelphia, PA 19104-6321

Please direct reprint requests and all correspondence to:

Susan Margulies
Department of Bioengineering
210 South 33rd St.
University of Pennsylvania
Philadelphia, PA 19104-6321
FAX 215 573 2071
PH 215 898 0882
Email margulie@seas.upenn.edu

Running Head: Stretch cycling frequency and magnitude affect epithelial permeability

Abstract

We measured stretch-induced changes in transepithelial permeability to uncharged tracers (1.5-5.5 Å) using cultured monolayers of alveolar epithelial type I “like” cells. Cultured alveolar epithelial cells were subjected to uniform cyclic (0, 0.25, and 1.0 Hz) biaxial stretch from 0% to 12%, 25%, or 37% change in surface area (ΔSA) for 1 hour.

Significant changes in permeability of cell monolayers were observed when stretched from 0% to 37% ΔSA at all frequencies, when stretched from 0% to 25% ΔSA only at high frequency (1 Hz), and not at all when stretched from 0 to 12% ΔSA compared to unstretched controls. Cells subjected to a single stretch cycle at 37% ΔSA (0.25 Hz), to simulate a deep sigh, were not distinguishable from unstretched controls. Reducing stretch oscillation amplitude while maintaining peak stretch of 37% ΔSA (0.25 Hz) via the application of a simulated post end expiratory pressure, or PEEP, did not protect barrier properties. At stretch oscillation amplitudes of 25 and 37% ΔSA , imposed at 1 Hz, tracer permeability increased compared to 0.25 Hz. We concluded that peak stretch magnitude and stretch frequency were the primary determining factors for epithelial barrier dysfunction, as opposed to oscillation amplitude.

Keywords: ventilator-induced lung injury, tight junction, barrier properties

Introduction

Ventilator induced lung injury (VILI), produced by cyclic over-inflation and collapse of airways and alveoli, is characterized by markers of reduced alveolar epithelial and/or endothelial barrier function such as air-leaks, pulmonary edema, and alveolar flooding (29).

A recent clinical study on ventilation strategies was carried out by the ARDSnet and showed mortality rates of patients with acute respiratory distress syndrome decreased significantly (22%) when a low ventilation volume (V_t , 6 ml/kg) compared to standard (12 ml/kg) V_t was used (2). Often, increased ventilation frequency is used to preserve minute ventilation at low tidal volumes and positive end-expiratory pressure (PEEP) is used to prevent alveolar collapse during mechanical ventilation. In the ARDSnet study ventilation frequency was controlled to maintain blood pH (7.3 – 7.4), and was approximately 0.5 Hz and 0.25 Hz for the low and high V_t groups, respectively (2). In addition, PEEP was maintained at approximately 8.5 and 9.4 cm H₂O for the low and high V_t groups group, respectively (2). It is possible that the higher PEEP used in the high V_t group may have contributed to the poor outcome.

A second ARDSnet clinical trial compared two PEEP levels (approximately 8 and 13 cm H₂O) at the same V_t (6.0 ml/kg), and revealed no protective or deleterious effects of increased PEEP for low stretch oscillation amplitude (SOA) ventilation (4). Rate was controlled to maintain a pH greater than 7.30 and averaged approximately 0.5 Hz for both groups. There are, however, questions about this second study, specifically concerning how study parameters were changed mid-trial yet all data was combined and used (19).

In summary, the use of PEEP is still a widely discussed issue, with greater than 280 publications on the subject in the last 2 years alone.

While both the epithelium and endothelium serve as barriers to particulate and fluid motion into the alveolus, the epithelium provides much more resistance to alveolar flooding (20). Previously, we presented a relationship between epithelial stretch and inspired lung volume in intact lungs (25). Here, we propose that both large stretch magnitudes and frequencies adversely affect epithelial barrier properties, including permeability.

We have developed an *in vitro* primary cell monolayer model of the alveolar epithelium that mimics lung inflation (25, 26). Briefly, equibiaxial stretch is applied to change the surface area of the monolayer at controlled frequencies and magnitudes. In a previous study, we cyclically stretched cultured monolayers at one stretch rate (0.25 Hz) to magnitudes of 25% or 37% ΔSA . We concluded that only epithelial deformation to magnitudes of 37% ΔSA , corresponding to 100% TLC, created a disruption of barrier properties to uncharged molecular tracers (radii 1.5-5.5 Å) (5, 25). This data concurred with findings by Egan and coworkers who showed that static inflation of whole sheep and rabbit lungs to 100% TLC produced permeability increases to tracers (radii 14-34 Å), while smaller inflations did not (11, 12).

In the current study, we use an our *in vitro* model to study the effects of mechanical stretch frequency, stretch oscillation amplitude, and peak stretch magnitude on barrier properties. To better understand the affect of PEEP on VILI, we applied a combination of tonic stretch (PEEP component) and cyclic stretch (ventilation component) to our isolated epithelial monolayers. These studies complement our

previous cell viability studies (27) and extend our previous functional studies (5) to investigate epithelial permeability under stretch conditions designed to mimic ventilation of the intact rodent respiratory system with moderate and high PEEP (at approximately 13 and 35 cm of H₂O) and higher frequencies of ventilation (1). Our results demonstrate that large peak stretch magnitude and high frequencies increase the flux of uncharged tracers into the alveolus, and that caution should be exercised when combining the two in a clinical setting.

Methods

Cell Isolation

Primary rat alveolar epithelial type II cells were isolated from pathogen-free male Sprague-Dawley rats (250-350 g) via an elastase digestion technique adopted from Dobbs *et. al.*(9). After isolation, cells were resuspended in a solution of minimum essential minerals (MEM), 10% fetal bovine serum, 0.4 µl/ml Gentamicin, and 1 µl/ml Amphotericin B (Life Technologies, Rockville, MD) and seeded (1×10^6 cells / cm²) on permeable co-polyester membranes (Mylan Technologies, Burlington, VT) mounted in custom-built polysulfone wells. The membrane was previously corona discharge-treated, and coated with poly-L-lysine (0.5 µg/cm²; Sigma, St. Louis, MO) and fibronectin (10 µg/cm²; Boehringer Mannheim Biochemicals, Indianapolis, IN) to improve cell adhesion. Wells were incubated for a period of 5 days, during which the media was changed daily. Other labs and we have shown previously that by 5-6 days in culture, type II alveolar epithelial cells seeded on fibronectin and maintained with 10% fetal bovine serum adopt type I features (7, 10, 21, 26). Others have noted that permeable supports encourage

emergence of type I features and non-permeable supports inhibit transformation (28). To confirm this phenotypic transformation, even on our elastic impermeable construct, we embedded cells in Epon A12 (Electron Microscopy Supply, Port Washington) and sectioned (60 – 85 nm). The cells were examined using electron microscopy after 2 and 5 days in culture (Figure 1). While cells at day 2 (upper left, Figure 1) contain numerous lamellar bodies, by day 5 cells seeded on our fibronectin-coated elastic substrate have formed monolayers and phenotypical characteristics of type I cells, including tight-junctions (upper right, Figure 1) and loss of lamellar bodies (center, Figure 1). Furthermore, cells seeded on fibronectin-coated permeable constructs develop transepithelial resistances averaging 800-1000 $\Omega\text{-cm}^2$, values representative of properly formed confluent alveolar monolayers (8, 15).

Cell Monolayer Stretching Protocol

Wells were washed with Ringer's solution (in mM: NaCl 126.4, NaHCO_3 25, HEPES 15, glucose 5.55, KCl 5.4, CaCl_2 1.8, MgSO_4 0.81, NaH_2PO_4 0.78; pH = 7.4) and mounted in a custom-made stretch device capable of applying a uniform and equibiaxial stretch to the cells at a user-defined magnitude and frequency (26). In a 3x3 design, wells were stretched at one of three frequencies (1 Hz, 0.25 Hz, or 0 Hz) and at one of three magnitudes (12%, 25%, 37% ΔSA) for 1 hour. We define 0 Hz as a prolonged constant stretch held for 1 hour. These three stretch magnitudes correspond to the strains experienced by the alveolar epithelium *in vivo* at inflations from functional residual capacity to 70%, 90% and 100% total lung capacity (TLC), or tidal volumes of 15, 25, and 30 ml/kg in the rat with no PEEP, respectively (25). Additional wells were stretched

cyclically (0.25 Hz) from 12% to 25% Δ SA or from 25% to 37% Δ SA for 1 hour, corresponding to lung stretch *in vivo* from 70% to 90% TLC and from 90% to 100% TLC, respectively. In animals with an intact chest wall, these two stretch paradigms would be associated with PEEP – SOA combinations of approximately 13 cm of H₂O – 10 ml per kg body weight, and 35 cm of H₂O – 5 ml per kg body weight, respectively in the rat (24). The final experimental group was subjected to a single stretch of 37% Δ SA at a frequency of 0.25 Hz to elicit the effect of a large “sigh” to TLC (with 2 sec inspiration, 2 sec expiration). The remainder of the wells were left unstretched in the device to serve as unstretched, time-matched controls. A total of 24 wells were used at each stretch condition for each tracer. The temperature of the stretch device was maintained at 37°C.

Cell Monolayer Tracer Transport Measurements

After the 1 hour experimental period, wells were removed from the stretch device and mounted into Ussing chambers within approximately 2 minutes. The apical to basal paracellular permeability of the monolayers was assessed using a previously described tracer transport methods (5). Briefly, five dextrorotary oligopeptide tracers were used to measure permeability: alanine (molecular radius = 2.2 Å), valine (2.8 Å), alanine-alanine (Ala-al; 3.6 Å), alanine-alanine-alanine (Ala-al; 4.4 Å), and leucine-leucine (Leu-leu; 5.5 Å). Tracer radius was estimated from molecular models obtained from the Protein Data Bank (www.umass.edu/microbio/rasmol/). Tracer transport in the apical-to-basal direction was measured over a 2 hour period, using a separate tracer for each well. Tracer samples (100 µl) were removed from the basal chamber every 30 minutes and

replaced with fresh Ringer's solution. Tracer concentrations were assessed by mixing a basal fluid sample with fluorescamine and quantifying the fluorescence using a microplate fluorimeter (Thermo Labsystems, Vantaa, Finland) with an excitation filter of 405 nm and an emission filter of 485 nm.

We assumed diffusive paracellular transport of tracers, with no sources or sinks, and used well-established equations governing conservation of mass (16, 18). Transport for each tracer followed first-order Fickian diffusion described by:

$$\ln \left(\frac{C_{A0} - \left(1 + \frac{V_B}{V_A}\right) C_B(t)}{C_{A0} - \left(1 + \frac{V_B}{V_A}\right) C_{B0}} \right) = - \frac{\left(1 + \frac{V_B}{V_A}\right) PS}{V_B} (t - t_0) \quad (1)$$

where C_{A0} = initial apical tracer concentration, C_{B0} = initial basal tracer concentration, $C_B(t)$ = basal concentration at time t , P = paracellular permeability of the monolayer to a specific tracer (units = length/time), S = surface area over which transport occurs, t_0 = initial time, V_A = apical volume, and V_B = basal volume. P was calculated over each of the four post-stretch or post-control periods ($t = 30, 60, 90$, and 120 min), and modeled as a piecewise continuous function. Tukey test for significance determined that tracer permeability was not a function of the time at which the sample was drawn (30), and P values determined from samples across time were averaged to yield P values for each tracer (for each well) as a result of the applied stretch regimen.

Calculation of equivalent pore radius

The calculated permeability values for all the tracers were used to develop a model of the equivalent pore radii of the epithelium as a function of applied stretch as previously

described (6). Based on the 2 pore model by Kim and Crandall (3, 17), paracellular tracer flux can be represented as:

$$PS = D[(A_{PS}/dx)f(a/r_s) + (A_{PL}/dx)f(a/r_L)] \quad (2)$$

where D is the diffusion coefficient of the tracer in water, A_P is the total pore area of the membrane, dx is the length of the cylindrical pores, a is the tracer radius, r is the pore radius, and P and S are defined as in Eq. 1. The polynomial function $f(a/r)$ is defined as $f(a/r) = (1 - a/r^2)(1 - 2.10a/r + 2.09a/r^3 - 0.95a/r^5)$, and represents the steric hindrance to molecular diffusion. To compute the pore radii, we first defined Alanine-alanine (3.6 Å) as our reference tracer based on observations from previous calculations using a single pore model, and used permeability data for tracers greater than or equal to the reference to solve for larger pore radii, and permeability data for tracers smaller than the reference to solve for small pore radii. Furthermore, we assumed that the large tracers were unable to pass through small pores, and therefore could neglect large tracer transport through the small pores when solving for large pore radii. In addition, A_{PL} and A_{PS} were calculated from these equations using the calculated pore radii and the reference permeability value. The number of pores was calculated using the formula

$$n = A_{PL}/\pi r_L^2 \text{ for large pores, and } n = A_{PS}/\pi r_s^2 \text{ for small pores.}$$

Statistical Analysis

To determine the effect of stretch frequency on paracellular permeability in cultured monolayers, separate permeability analyses for each tracer were performed, comparing across frequencies at a particular stretch magnitude using ANOVA. Subsequently, post

hoc Tukey tests were used for multiple comparisons (30) (JMP 4, (SAS Institute, Cary, NC)). Statistical significance was defined as $p \leq 0.05$.

Specifically, *in vitro* monolayer tracer permeabilities measured in the 12 – 25% Δ SA and 25 – 37% Δ SA stretch groups (0.25 Hz), were compared with each other and previously obtained tracer data from a 0.25 Hz 0 - 12% Δ SA stretch group (0.25 Hz) (5) (Tukey test) to evaluate differences between these three stretch strategies that employed 12-13% Δ SA cyclic SOAs.

The final analysis of the *in vitro* monolayer data was used to determine whether the peak deformation magnitude or the SOA of stretch is the main determinant of barrier disruption in these cells. The 12 – 25% Δ SA (0.25 Hz) group was compared to the previously obtained 0 – 25% Δ SA (0.25 Hz) group using unpaired Student's test (30). Similarly, data from the 25 – 37% Δ SA (0.25 Hz) stretch group were compared to those of the previously examined 0 – 37% Δ SA (0.25 Hz) group to examine the same phenomena at higher stretch magnitudes.

Results

In previous studies (5), we showed that paracellular permeability of cultured alveolar epithelial cells stretched cyclically at 0.25 Hz significantly increased compared to unstretched cells, but only with a stretch from 0 to 37% Δ SA, not with 0 to 25% Δ SA. We concluded that at stretch magnitudes at or greater than 37% Δ SA (100% TLC), sustained low frequency cycling can damage barrier properties.

In the current study, we used the same tracers to evaluate the effect of mechanical conditions analogous to clinical ventilation paradigms on epithelial permeability. We

found that increasing stretch cycling frequency to 1 Hz increased the permeability of cultured monolayers stretched from 0 to 37% Δ SA (◆, Figure 3). Specifically, passive transport of all tracers through monolayers stretched from 0 to 37 % Δ SA at 1 and 0.25 Hz was significantly greater than that through unstretched monolayers, and transport at 1 Hz was also significantly greater than passive transport of most tracers under 0 Hz stretch to 37% Δ SA (**, Figure 3). Moreover, for cyclic stretch from 0 to 37 Δ SA, permeability at 1 Hz was even significantly greater than stretch at 0.25 Hz for two tracers (*, Figure 3). Even a 0 Hz stretch held at 37% Δ SA for 1 hour significantly increased the permeability of valine (2.8 Å) and alanine-alanine (3.6 Å) compared to unstretched monolayers (†, Figure 3). Whereas sustained 0 Hz and cyclic stretch to 37% Δ SA can damage barrier properties, we find that a single “sigh”, one brief stretch at a rate of 0.25 Hz to 37% Δ SA (100% TLC or 30 ml/kg in the rat), did not significantly increase the permeability of cell monolayers to any of the tracers (Δ , Figure 3) compared to unstretched controls.

Similar to stretch at 37% Δ SA, permeability of monolayers stretched to 25% Δ SA at a frequency of 1 Hz was also significantly greater than unstretched cells for all tracers (Figure 4), and even greater than the permeability of monolayers stretched at 0 Hz or 0.25 Hz at 25% Δ SA for all but the smallest tracer (*, Figure 4). From our data at both 25% and 37% Δ , we conclude that stretch frequency is an important determinant of barrier dysfunction at or above 25% Δ SA (90% TLC or 25 ml/kg in the *in vivo* rat).

To determine if sustained cycling from a minimum, non-zero, stretch magnitude compromised barrier properties of monolayers exposed to small (12 or 13% Δ SA) SOAs, we examined permeability of monolayers cycled at either 12 - 25% Δ SA or 25 - 37% Δ SA (0.25 Hz) and compared their values to those of monolayers cycled at the same

SOA (0 - 12% Δ SA), but with no pre-stretch or PEEP (■, Figure 5). Assuming this minimum stretch magnitude of 12% Δ SA is like an “end-expiratory stretch”, this magnitude corresponds to an end expiratory pressure approximately equivalent to 13 cm of H₂O in the intact respiratory system (25). The combination of this moderate, non-zero minimum stretch (PEEP) with a SOA from 70 to 90 %TLC (10 ml/kg in the rat) did not alter monolayer permeability to any tracer (Δ Figure 5, 12-25% Δ SA). However, in the 25 to 37% Δ SA group the combination of a minimum stretch of 25% Δ SA (or PEEP of 35 cm H₂O in the intact respiratory system) with a SOA from 90 to 100% TLC (5 ml/kg in the rat), which is independently a non-injurious SOA, did significantly increase permeability to all tracers (\diamond Figure 5, 25-37% Δ SA). However, when SOA was reduced to zero and the same large PEEP equivalent stretch (25% Δ SA) was applied and held at constant (0 Hz) stretch for 1 hour (■, Figure 4), permeability did not increase relative to unstretched controls. Thus we conclude that PEEP alone was not the cause of the increased permeability of monolayers stretched from 25 to 37% Δ SA, but rather peak stretch magnitude was primarily responsible. Permeability increased significantly only when maximum stretch reached 37% Δ SA (or 100% TLC) either tonically or dynamically.

To determine if SOA affected the influence of peak stretch magnitude on permeability, we examined two sets of data in Figure 5 comparing conditions with matched maximum stretch at a frequency of 0.25 Hz: 12 - 25% Δ SA with 0 - 25% Δ SA, and 25 - 37% Δ SA with 0 - 37% Δ SA. No significant differences were found between groups stretched to the same peak magnitude.

As a theoretical basis for interpreting the changes in monolayer permeability following stretch, we modeled the monolayers as an impermeable sheet with two populations of pores, a large radius and small radius population, available for tracer transport. The model was fit to permeability data obtained from each of our 5 tracers following each stretch regimen, and pore radii, total pore area, and pore number were calculated (Table 1). In a previous study, we used this model to show that following a cycling rate of 0.25 Hz, only stretch to 37% Δ SA produced increases in small (2 fold) and large (9 fold) pore radius compared to unstretched values (6). Furthermore, at this stretch magnitude and rate we reported a decrease in total area occupied by small pores (to 32% of unstretched) and an increase in the total area of large pores (to 1976% of unstretched). In the present study at the same rates and magnitudes we see an increase in the total area occupied by both small and large pores, but again the large pore area increased most, with dramatic increases at 37% Δ SA.

Here we also examined high rates of cyclic stretch (1.0 Hz) to 25% and 37% Δ SA, as well as the effect of cyclic stretch with “PEEP” (12-25% and 25-37% Δ SA at 0.25 Hz). Comparing stretch at 37% Δ SA at 1.0 Hz to 0.25 Hz, both small and large pore size increased, but increases in total small pore area were smaller (2 and 4 fold) than large pore area (39 and 22 fold compared to unstretched monolayers). The further increase in permeability for small tracers seen by increasing the rate to 1.0 Hz (Figure 2) seems to be related to increases in total area of the large pores. This relationship also holds at 25% Δ SA, where the large and small pore area increases are less than at 37% Δ SA at the same frequencies, but again the significant increase in large and small tracer permeability at 1.0 Hz (Figure 3) seems to correlate with the 12 fold increase in the total

area of large pores. Thus, the model simulation suggests that the formation of large pores is responsible for the increases in measured monolayer permeability.

The pore model was also used to interpret the permeability data from the PEEP studies at 0.25 Hz (Figure 4). Stretch to peak amplitude of 25% ΔSA (Table 1: 25% and 12-25%) led to modest increases in total area of small and large pores, and no significant increase in permeability (Figure 4). Stretch to peak magnitude of 37% ΔSA (Table 1: 37% and 25-37%) produced increases in total area occupied by small pores, and dramatically larger increases in the total area occupied by large pores (18-22 fold increases above unstretched monolayers). Again, these data concur with a correlation between significant increases in monolayer permeability (Figure 4) and the total area of the large pores. Finally, the large pore area changes also demonstrate that stretch to a magnitude of 37% ΔSA produces profound large pore area change, even with a reduced stretch amplitude.

Discussion

Previously, we have shown that subjecting cultured alveolar epithelial cell monolayers to large cyclic stretch for 1hr and a rate of 0.25 Hz increases paracellular tracer flux (5). Specifically, we found that increasing stretch oscillation amplitude increased monolayer permeability in a non-linear manner, such that amplitudes around TLC produced dysfunction. In this study, we examine the effect of increased cycling frequency (1.0 Hz), and separately address the influence of stretch oscillation amplitude and peak stretch magnitude on epithelial permeability. Our results indicate that within the physiological range, both the peak stretch magnitude and the cycling frequency affect

the extent of stretch-induced barrier dysfunction. Specifically, reductions in stretch oscillation while maintaining the same peak stretch magnitude did not produce significant functional improvements. Combined with our previous studies (5), we now conclude that the maximum magnitude of stretch rather than SOA (difference between the maximum and minimum stretch in the cycle, equivalent to tidal volume) produces epithelial barrier dysfunction in sustained cyclic or tonic (0 Hz) mechanical stretch environments.

Furthermore, we demonstrate brief exposures to the same peak stretch magnitude (similar to a deep sigh), does not alter barrier properties. These findings show that caution should be exercised when using large PEEP levels in conjunction with even small tidal volumes, because repetition of high peak deformations could result. The data at large peak stretch levels support the analysis of Hager *et. al.* who evaluated animal and clinical data and reported significant reductions in mortality by decreasing peak inspiratory plateau pressure (14). However, Hager *et. al.* also note further reductions in mortality by reducing tidal volume at high plateau pressures, and more modest effects at lower peak pressures. Perhaps differences between *in vitro* and *in vivo* platforms and due to differences in the readout, namely permeability vs. mortality.

The observed frequency dependence of cell monolayer permeability is comparable to cell death results reported by Tschumperlin *et. al.* in which post-stretch cell viability in 5 day rat alveolar epithelial cells was measured using a plasma membrane rupture assay (27). In that study, cell death after stretch at 50% ΔSA increased as the applied stretch frequency was increased. However, Tschumperlin *et. al.* observed no significant cytotoxicity with high deformation magnitudes to 100% TLC, as long as the frequency of stretch remained small (0.25 Hz). Our present work has shown that barrier

function in the same cultured monolayer preparation is compromised by high peak deformation magnitude even at modest stretch frequency (0.25 Hz). Thus, we find that stretch thresholds for barrier dysfunction are lower than those for cell death.

The differing effect of stretch frequency on cell death and epithelial permeability may be due to cellular regulation of the plasma membrane. As inferred by capacitance data presented by Fisher *et. al*, the plasma membrane of cultured alveolar epithelial cells is enlarged via lipid trafficking within 5 minutes of the application of 0 Hz stretch to peak basal membrane deformations of 25% ΔSA (13). It is most likely the case that as stretch frequency increases, the rate of lipid trafficking to the cell membrane is not high enough to support large magnitudes of deformation, which leads to membrane rupture and cell death. Furthermore, we have shown that at a stretch magnitude of 25% ΔSA and all frequencies, the actin cytoskeleton is reorganized with a concentration at cortical cell boundaries (23). Therefore, we speculate increases in paracellular permeability without increases in cell mortality at low stretch frequencies could be explained by a sufficient rate of lipid insertion into the plasma membrane to limit cell death, however, concurrent rearrangement of the actin cytoskeleton and junctional proteins result in functional alterations, such as permeability increases.

Alternatively, high frequency cyclic stretch could lead to increases in epithelial permeability through mechanical failure of the cell-cell junction. As cycling frequency increases, the rate of cellular stretch increases and magnifies the forces experienced by the cells and their junctions in a non-linear manner due to the viscoelastic nature of the cells. It is possible that at higher frequencies, there is a higher incidence of cell death that could lead to hole formation in the monolayer. We performed live/dead staining on a

small number of stretched monolayers, and while there were a higher percentage of dead cells in monolayers stretched at a higher frequency, the dead cells were still adherent to the monolayer, but may have dissociated from neighboring cells. In previous studies, we have shown that the loss of junctional integrity leads to increases in permeability similar to stretch at 0.25 Hz to 37% Δ SA, but the monolayer is still significantly less permeable than bare membrane (6). Therefore, a second mechanism underlying stretch induced barrier dysfunction could be a mechanical failure of the cell-cell junction due to the development of high viscous forces produced by the increased cycling frequency.

One methodological limitation of our study may be the possible recovery or worsening properties of the epithelial barrier during the 2 hour time period between stretch completion and the end of the transport tests. Although proteins in stable junctional complexes have been shown to cycle from the cytoplasm to the membrane on the order of minutes (22), others demonstrate a 4 hour lag time between a calcium switch to initiate barrier formation, and development of functioning barriers in MDCK cells (31). In our previous studies, we monitored the permeability of the monolayers every 15 minutes for 2 hours following stretch and found that there was no significant change in monolayer permeability over the time period (6). Thus we conclude it is unlikely that the junctions undergo significant repair or deterioration during the 2 hour period of measurement.

A second limitation of this study is that the period of study was only 60 minutes, focusing on acute changes in barrier function. In contrast, mechanical ventilation is usually employed for hours or days at a time in the clinical setting, providing a longer time period over which epithelial dysfunction could develop. While we observed

changes after an hour of applying some stretch regimens, it may be possible that the regimens that did not produce any measurable changes in the hour stretch period may produce significant barrier disruption after a longer stretch duration. Conversely, it is possible that the cells will adapt to the applied stretch conditions over prolonged stretch periods. In this case, we would expect a reduction of epithelial permeability following epithelial adaptation. The contribution of longer stretch durations should be addressed in future studies. Finally, the relationships between lung volume (TLC) and epithelial deformation used in this manuscript are based on data obtained by deflating isolated lungs from TLC in a quasi-static manner prior to fixation. It is possible that dynamic lung ventilation *in situ* alters the spatial distribution and magnitude of alveolar epithelial stretch magnitude.

In summary, we use a homogeneous alveolar epithelial cell monolayer to identify limits of end-expiratory volume, stretch magnitude and frequency associated with acute changes in epithelial barrier function. These data provide a foundation of functional thresholds that we and others can use in the future to develop experimental designs to investigate the mechanics underlying stretch-induced epithelial disruption.

References

1. **Agostoni E, and Mead J.** Statics of the respiratory system. In: *Handbook of Physiology: Respiration*, edited by Wallace O. Fenn HR. Washington, D.C.: American Physiological Society, 1964, p. 387-410.
2. **Anonymous.** Ventilation with lower tidal volumes as compared with traditional tidal volumes for acute lung injury and the acute respiratory distress syndrome. . *N Engl J Med* 342: 1301-1308, 2000.
3. **Berg MM, Kim KJ, Lubman RL, and Crandall ED.** Hydrophilic solute transport across rat alveolar epithelium. *J Appl Physiol* 66: 2320-2327, 1989.
4. **Brower RG, Lanken PN, MacIntyre N, Matthay MA, Morris A, Ancukiewicz M, Schoenfeld D, and Thompson BT.** Higher versus lower positive end-expiratory

pressures in patients with the acute respiratory distress syndrome. *N Engl J Med* 351: 327-336, 2004.

5. **Cavanaugh Jr KJ, Cohen TS, and Margulies SS.** Stretch Increases Alveolar Epithelial Permeability to Uncharged Micromolecules. *Am J Physiol Cell Physiol* 2005.
6. **Cavanaugh KJ, Cohen TS, and Margulies SS.** Stretch increases alveolar epithelial permeability to uncharged micromolecules. *Am J Physiol Cell Physiol* 290: C1179-1188, 2006.
7. **Cheek JM, Evans MJ, and Crandall ED.** Type I cell-like morphology in tight alveolar epithelial monolayers. *Exp Cell Res* 184: 375-387, 1989.
8. **Cheek JM, Kim KJ, and Crandall ED.** Tight monolayers of rat alveolar epithelial cells: bioelectric properties and active sodium transport. *Am J Physiol* 256: C688-693, 1989.
9. **Dobbs LG, Gonzalez R, and Williams MC.** An improved method for isolating type II cells in high yield and purity. *Am Rev Respir Dis* 134: 141-145, 1986.
10. **Dobbs LG, Williams MC, and Gonzalez R.** Monoclonal antibodies specific to apical surfaces of rat alveolar type I cells bind to surfaces of cultured, but not freshly isolated, type II cells. *Biochim Biophys Acta* 970: 146-156, 1988.
11. **Egan EA.** Lung inflation, lung solute permeability, and alveolar edema. *J Appl Physiol* 53: 121-125, 1982.
12. **Egan EA.** Response of alveolar epithelial solute permeability to changes in lung inflation. *J Appl Physiol* 49: 1032-1036, 1980.
13. **Fisher JL, Levitan I, and Margulies SS.** Plasma membrane surface increases with tonic stretch of alveolar epithelial cells. *Am J Respir Cell Mol Biol* 31: 200-208, 2004.
14. **Hager DN, Krishnan JA, Hayden DL, and Brower RG.** Tidal volume reduction in patients with acute lung injury when plateau pressures are not high. *Am J Respir Crit Care Med* 172: 1241-1245, 2005.
15. **Kim KJ, Borok Z, Ehrhardt C, Willis BC, Lehr CM, and Crandall ED.** Estimation of paracellular conductance of primary rat alveolar epithelial cell monolayers. *J Appl Physiol* 98: 138-143, 2005.
16. **Kim KJ, and Crandall ED.** Effects of lung inflation on alveolar epithelial solute and water transport properties. *J Appl Physiol* 52: 1498-1505, 1982.
17. **Kim KJ, and Crandall ED.** Heteropore populations of bullfrog alveolar epithelium. *J Appl Physiol* 54: 140-146, 1983.
18. **Kim KJ, LeBon TR, Shinbane JS, and Crandall ED.** Asymmetric [14C]albumin transport across bullfrog alveolar epithelium. *J Appl Physiol* 59: 1290-1297, 1985.
19. **Levy MM.** PEEP in ARDS--how much is enough? *N Engl J Med* 351: 389-391, 2004.
20. **Lubman RL KK, Crandall ED.** Alveolar Epithelial Barrier Properties. In: *The Lung: Scientific Foundations*, edited by RG C, and JB W. Philadelphia: Lippincott-Raven, 1997, p. 585-602.
21. **Qiao R, Zhou B, Liebler JM, Li X, Crandall ED, and Borok Z.** Identification of three genes of known function expressed by alveolar epithelial type I cells. *Am J Respir Cell Mol Biol* 29: 98-105, 2003.

22. **Shen L, Weber CR, and Turner JR.** The tight junction protein complex undergoes rapid and continuous molecular remodeling at steady state. *J Cell Biol* jcb.200711165, 2008.
23. **SS Margulies KC, TS Cohen, BC DiPaolo.** High Stretch Cycling Rates Alter Alveolar Epithelial Permeability and Actin Organization. In: *American Thoracic Society International Conference*. San Diego, Ca: The American Thoracic Society, 2005, p. A826.
24. **Stahl WR.** Scaling of respiratory variables in mammals. *J Appl Physiol* 22: 453-460, 1967.
25. **Tschumperlin DJ, and Margulies SS.** Alveolar epithelial surface area-volume relationship in isolated rat lungs. *J Appl Physiol* 86: 2026-2033, 1999.
26. **Tschumperlin DJ, and Margulies SS.** Equibiaxial deformation-induced injury of alveolar epithelial cells in vitro. *Am J Physiol* 275: L1173-1183, 1998.
27. **Tschumperlin DJ, Oswari J, and Margulies AS.** Deformation-induced injury of alveolar epithelial cells. Effect of frequency, duration, and amplitude. *Am J Respir Crit Care Med* 162: 357-362, 2000.
28. **Wang F, Daugherty B, Keise LL, Wei Z, Foley JP, Savani RC, and Koval M.** Heterogeneity of claudin expression by alveolar epithelial cells. *Am J Respir Cell Mol Biol* 29: 62-70, 2003.
29. **Webb HH, and Tierney DF.** Experimental pulmonary edema due to intermittent positive pressure ventilation with high inflation pressures. Protection by positive end-expiratory pressure. *Am Rev Respir Dis* 110: 556-565, 1974.
30. **Zar J.** *Biostatistical Analysis*. Upper Saddle River, NJ: Prentice Hall, 1999.
31. **Zheng B, and Cantley LC.** Regulation of epithelial tight junction assembly and disassembly by AMP-activated protein kinase. *Proc Natl Acad Sci U S A* 104: 819-822, 2007.

Table Captions

Table 1: Results of a 2 pore model of epithelial monolayer permeability, for either unstretched cells, or stretch at 0.25 Hz (0% to 25%, 0% to 37%, 12% to 25%, and 25% to 37% Δ SA) or 1.0 Hz (0% to 25% and 0% to 37% Δ SA).

		No Stret ch	0.25 Hz				1.0 Hz	
			25%	12-25%	37%	25-37%	25%	37%
Small Pore s	Radius, Å	3.06	3.04	3.44	2.649	3.44	3.44	3.44
	Number, billion	636	889	401	3370	616	572	1070
	Pore Area, billion nm ²	187	258	149.1	743	229	212	398
Large Pore s	Radius, Å	31.2	31.2	27.5	39.6	35.7	33.4	40.5
	Number, thousand	444	579	782	6070	5990	4820	10310
	Pore Area, million nm ²	13.59	17.6 5	18.59	299	240	168.7	532

Table 1: Results of a 2 pore model of epithelial monolayer permeability, for either unstretched cells, or stretch at 0.25 Hz (0% to 25%, 0% to 37%, 12% to 25%, and 25% to 37% Δ SA) or 1.0 Hz (0% to 25% and 0% to 37% Δ SA).

Figure Captions

Figure 1: Electronmicrographs (obtained at 10,000x) of rat alveolar type II cells seeded on fibronectin-coated elastic substrate and maintained for 2 days in culture (top left) show numerous lamellar bodies (LB). After 5 days in culture, cells take on an alveolar type I “like” phenotype (lower center) with no lamellar bodies but the formation of tight junctions (TJ, 150,000x, top right).

Figure 2: Permeability of monolayers stretched to 37% Δ SA at frequencies ranging from 0 to 1 Hz. For cells stretched at 1 Hz, tracer permeabilities significantly different from those of the unstretched group and the 0 Hz group are indicated by ** ($p < 0.05$), while those different from the unstretched group and the 0 Hz and 0.25 Hz groups are represented by * ($p < 0.05$). Unstretched and 0.25 Hz data presented previously (5). For the 0 Hz group, tracer permeabilities that differ from those of unstretched cells are indicated by † ($p < 0.05$). Tracers: alanine (2.2Å), valine (2.8Å), alanine-alanine (3.6Å), alanine-alanine-alanine (4.4Å), leucine-leucine (5.5Å).

Figure 3: Permeability of monolayers stretched to 25% Δ SA at frequencies ranging from 0 to 1 Hz. Tracer permeabilities that differ from those of unstretched cells and the cells stretched at 0 and 0.25 Hz are indicated by * ($p < 0.0001$). Unstretched and 0.25 Hz data presented previously (5). Tracers: alanine (2.2Å), valine (2.8Å), alanine-alanine (3.6Å), alanine-alanine-alanine (4.4Å), leucine-leucine (5.5Å).

Figure 4: Influence of minimum stretch magnitude on permeability of monolayers stretched cyclically. For cells stretched between 25% and 37% Δ SA, tracer permeabilities significantly different from those of the 0 - 12% Δ SA group and the 12 - 25% group are indicated by * ($p < 0.005$). Tracers: alanine (2.2Å), valine (2.8Å), alanine-alanine (3.6Å), alanine-alanine-alanine (4.4Å), leucine-leucine (5.5Å).

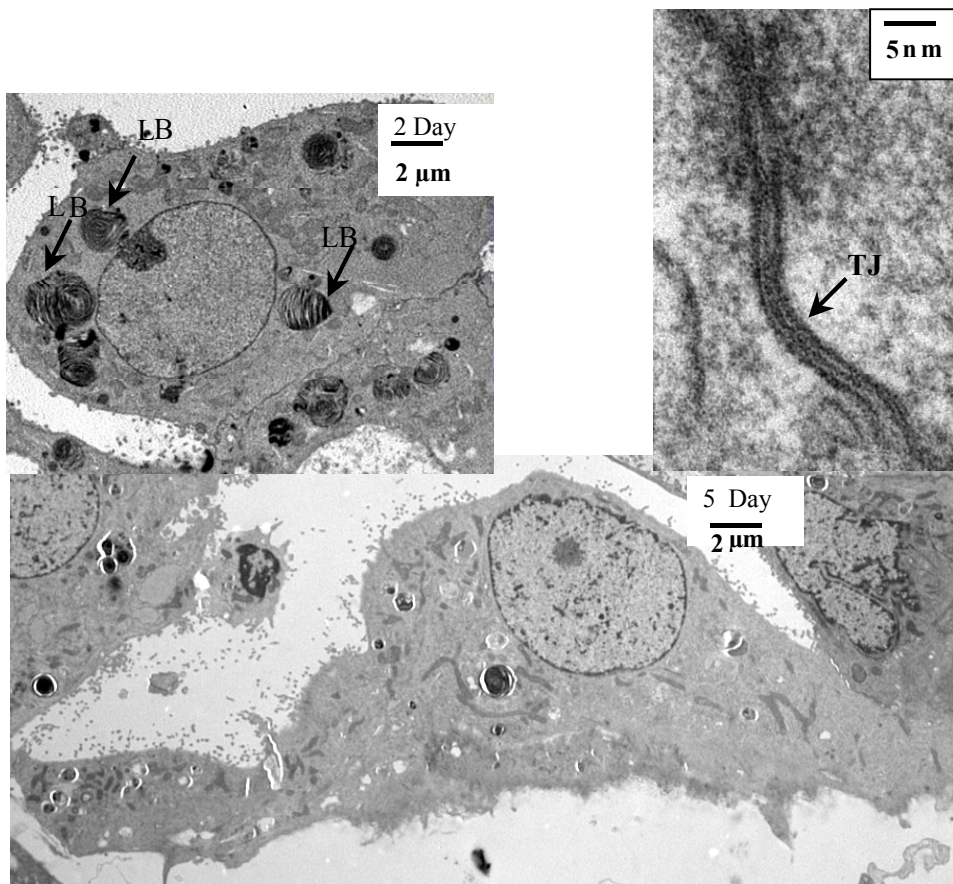


Figure 1: Electronmicrographs (obtained at 10,000x) of rat alveolar type II cells seeded on fibronectin-coated elastic substrate and maintained for 2 days in culture (top left) show numerous lamellar bodies (LB). After 5 days in culture, cells take on an alveolar type I “like” phenotype (lower center) with no lamellar bodies but the formation of tight junctions (TJ, 150,000x, top right).

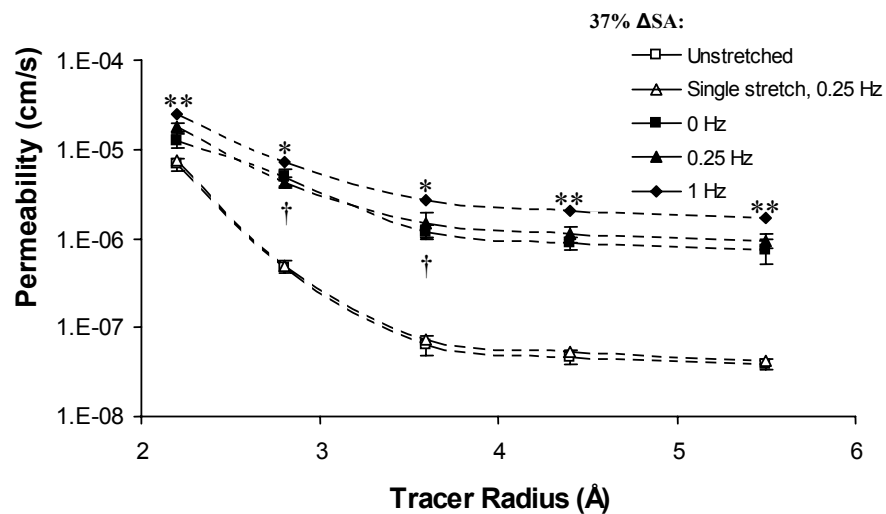


Figure 2: Permeability of monolayers stretched to 37% Δ SA at frequencies ranging from 0 to 1 Hz. For cells stretched at 1 Hz, tracer permeabilities significantly different from those of the unstretched group and the 0 Hz group are indicated by ** ($p < 0.05$), while those different from the unstretched group and the 0 Hz and 0.25 Hz groups are represented by * ($p < 0.05$). Unstretched and 0.25 Hz data presented previously (5). For the 0 Hz group, tracer permeabilities that differ from those of unstretched cells are indicated by † ($p < 0.05$). Tracers: alanine (2.2Å), valine (2.8Å), alanine-alanine (3.6Å), alanine-alanine-alanine (4.4Å), leucine-leucine (5.5Å).

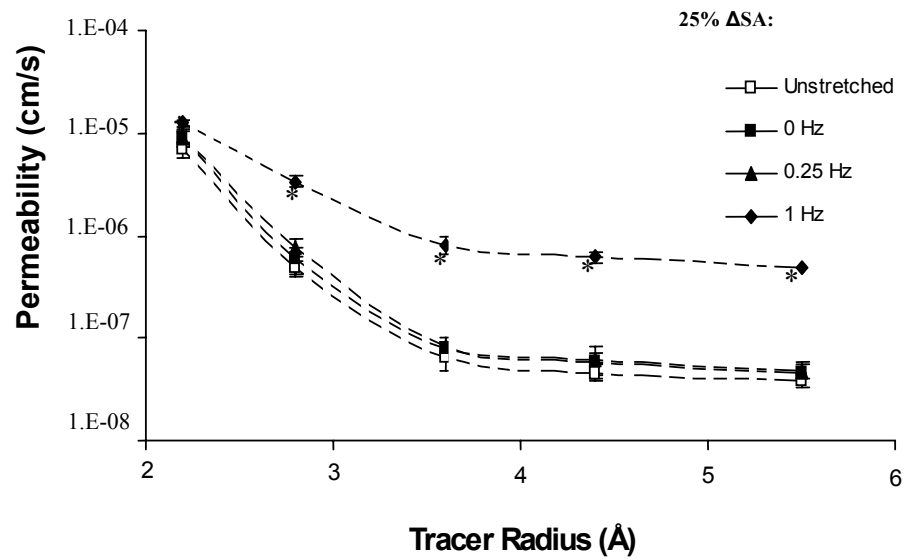


Figure 3: Permeability of monolayers stretched to 25% ΔSA at frequencies ranging from 0 to 1 Hz. Tracer permeabilities that differ from those of unstretched cells and the cells stretched at 0 and 0.25 Hz are indicated by * ($p < 0.0001$). Unstretched and 0.25 Hz data presented previously (5). Tracers: alanine (2.2Å), valine (2.8Å), alanine-alanine (3.6Å), alanine-alanine-alanine (4.4Å), leucine-leucine (5.5Å).

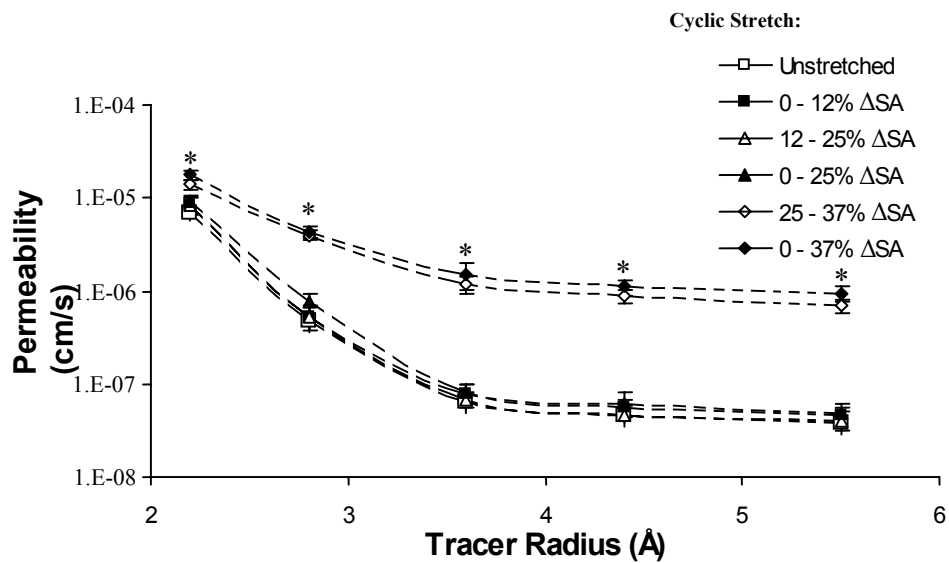


Figure 4: Influence of minimum stretch magnitude on permeability of monolayers stretched cyclically. For cells stretched between 25% and 37% ΔSA , tracer permeabilities significantly different from those of the 0 - 12% ΔSA group and the 12 - 25% ΔSA group are indicated by * ($p < 0.005$). These data illustrate that maximum deformation, not deformation amplitude is relevant to epithelial barrier dysfunction. Tracers: alanine (2.2Å), valine (2.8Å), alanine-alanine (3.6Å), alanine-alanine-alanine (4.4Å), leucine-leucine (5.5Å).